Wu *et al. Biochar* (2025) 7:85
https://doi.org/10.1007/s42773-025-00478-8

Biochar

ORIGINAL RESEARCH

Open Access

Biochar conductivity enhances methane generation in paddy soil by facilitating electron transfer mediated by dissolved organic matter

Yufei Wu[1†], Ting He[1†], Chen Cheng[2], Bo Liu[1], Zhaofeng Chang[1], Wei Du[1], Hao Li[1], Peng Zhang[1*] and Bo Pan[1*]

Abstract

Biochar can regulate methane (CH_4) emissions from paddy soils. However, the mechanism through which biochar conductivity influences methanogenesis in paddy soils remains unclear. In this study, biochar samples with varying conductivity levels were prepared by incorporating different amounts of graphene. The dissolved organic matter (DOM) derived from biochar was completely eliminated before its application. The addition of conductive biochar in the paddy soil system increased CH_4 production by enhancing the electron transfer rate (ETR), as demonstrated by a significant positive correlation between CH_4 production and ETR. Electrochemical experiments conducted after the removal of DOM from paddy soil demonstrated that biochar enhanced the ETR in paddy soils by facilitating the electron transfer of dissolved organic matter. Anthraquinone-2,6-disulfonate (AQDS), a common analogue for quinone- and hydroquinone-containing molecules in DOM, facilitates electron transfer and serves as a model for electrochemically active DOM. An experiment with biochar and AQDS confirmed that biochar enhanced the ETR of AQDS, supporting previous findings. Following incubation, methanogenic archaea showed no significant change in relative abundance across systems, demonstrating that that biochar enhanced methanogenesis solely via accelerated ETRs, without altering the microbial community composition. This study deepens our understanding of how biochar conductivity affects methanogenesis and offers scientific guidance for optimising the use of biochar in paddy soils.

Highlights

- Biochar increased methane production in paddy soil by promoting the electron transfer.
- The electron transfer in paddy soil was mediated by dissolved organic matter.
- Biochar enhanced the electron transfer in paddy soil due to its conductivity.

Keywords Biochar, Conductivity, Methanogenesis, Dissolved organic matter, Electron transfer

†Yufei Wu and Ting He have contributed equally to this work.

*Correspondence:
Peng Zhang
da.feipeng@163.com
Bo Pan
panbocai@gmail.com
Full list of author information is available at the end of the article

Graphical Abstract

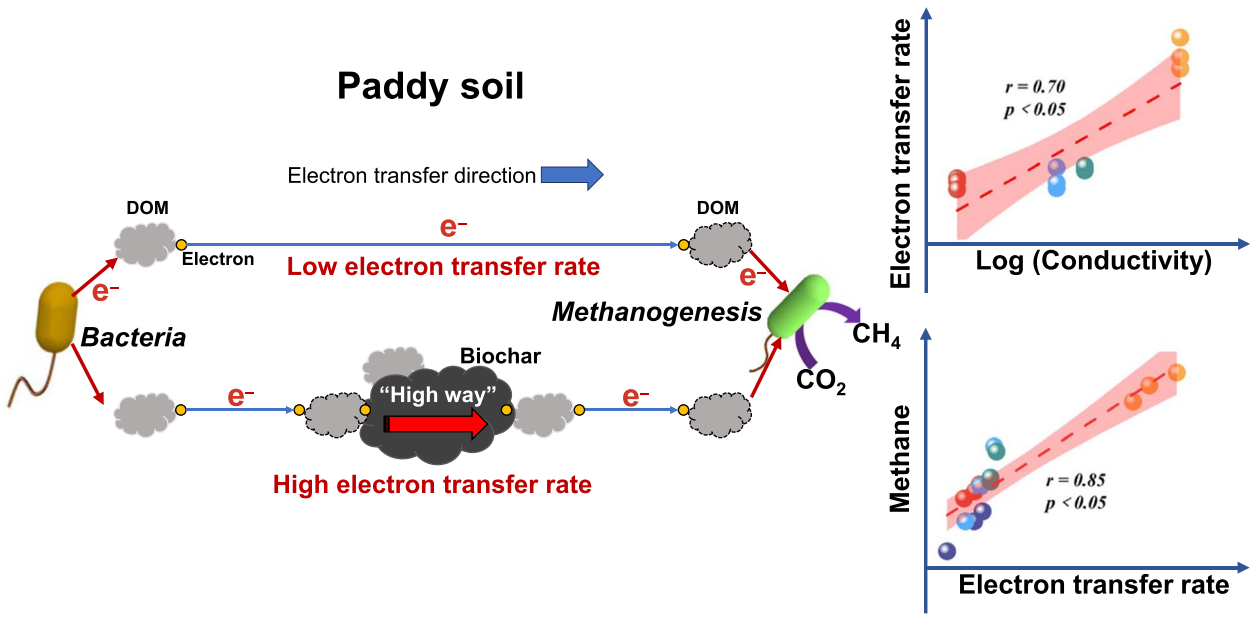

1 Introduction

Methane (CH_4), a potent greenhouse gas with a global warming potential 27.5 times greater than carbon dioxide (CO_2), persists in the atmosphere for about 12 years (Matthews and Wassmann 2003; Nan et al. 2021). Rice paddy soils, comprising approximately 9% of global cropland area, are a significant source of CH_4 emissions, contributing 30% of annual agricultural CH_4 emissions, estimated between 3.1×10^{10} kg and 11.2×10^{10} kg (Asadi et al. 2021; Ding et al. 2016; Nguyen et al. 2020; Qian et al. 2023). Therefore, it is crucial to investigate the biochemical processes associated with CH_4 emissions in paddy soils. Currently, four main methanogenesis mechanisms have been recognized: (1) Hydrogenotrophic: methanogens produce CH_4 using hydrogen (H_2) and CO_2 as substrates ($4H_2 + CO_2 \rightarrow CH_4 + 2H_2O$) (Leigh et al. 2011); (2) Acetoclastic: methanogens directly decompose acetic acid to produce CH_4 ($CH_3COOH \rightarrow CH_4 + CO_2$) (Thauer et al. 2008; Xiao et al. 2019); (3) Methylotrophic: methanogens utilize methyl groups in methyl compounds to produce CH_4 ($4\ CH_3OH \rightarrow 3\ CH_4 + CO_2 + 2H_2O$) (Makarova et al. 2007); (4) Electron-methanogenesis: electroactive microorganisms transfer electrons to methanogens, which then reduce CO_2 to generate CH_4 (Mand and Metcalf 2019; Rotaru et al. 2014; Xie et al. 2021).

Biochar is produced through the pyrolysis of various types of biomass under oxygen-limited or anaerobic conditions (Haris et al. 2021). This carbonaceous material exhibits certain conductive properties, which is related to its carbonization temperature. Biochar can donate and accept electrons through its numerous surface functional groups, thereby participating in environmental electron transfer processes. Given these characteristics, it is important to understand how biochar influences electron transfer in paddy soils and consequently affect CH_4 production.

Previous studies have reported conflicting results regarding the effects of biochar on methanogenesis. For instance, Nan et al. observed that the short-term application of low-concentration biochar (2.8 t ha^{-1}) reduced CH_4 emissions by 41% in paddy soils (Nan et al. 2020). Similarly, other studies have reported that the addition of biochar significantly reduces greenhouse gas emissions, including CH_4 (Qi et al. 2017; Uchimiya et al. 2011a, b). Conversely, numerous studies have indicated increased CH_4 emissions following biochar application. For example, Yang et al. found that biochar stimulated methanogenesis within a paddy soil enrichment culture (Yang et al. 2021). The conflicting results may stem from the diverse mechanisms through which biochar can influence microbial methane production in paddy soil.

Biochar can impact methane generation in paddy soil through several mechanisms. Firstly, biochar can provide dissolved organic matter components that microorganisms can metabolize, leading to increased oxygen consumption and enhanced CH_4 emissions (Ji et al. 2020;

Kubaczynski et al. 2023). Secondly, biochar can adsorb dissolved organic carbon in the soil, diminishing carbon sources available to soil microorganisms and inhibiting CH_4 production (Cavali et al. 2022; Jin et al. 2022). Lastly, the electron transfer capacities of biochar can facilitate electron transfer among different microorganism species, thereby influencing the overall CH_4 production (Wang et al. 2021; Zhang et al. 2021). Biochar can act as an electron transfer conduit, enhancing the electron transfer between fermentative bacteria and methanogens to facilitate electron-driven methanogenesis (Kim et al. 2022). The diverse effects of biochar on CH_4 production in paddy fields are influenced by various factors. Changes in the biochar preparation conditions result in alterations in characteristics like soluble organic matter content, adsorption properties, and conductivity. This simultaneous variability complicates the actual effects of biochar on microbial methanogenesis and hinders the precise interpretation of individual biochar factors on CH_4 production in paddy soil. Therefore, the specific role of biochar conductivity on CH_4 production in paddy soils is currently unclear and requires further investigation.

Therefore, in this study, we incorporated various quantities of graphene into sodium alginate to produce biochar with different conductivity levels, which were then added to a paddy soil system for anaerobic incubation. We measured the changes in gas generation and electron transfer rate (ETR) in all systems during incubation and analysed the bacterial and archaeal communities. This allowed us to investigate the effect of biochar conductivity on the methanogenic process of paddy soil and to elucidate the mechanism by which biochar conductivity regulates the methanogenic action of paddy soil.

2 Materials and methods

2.1 Model biochar production and characterization

Sodium alginate solutions (10 g L^{-1}, 250 mL) with different amounts of graphene (0, 10, 20, and 40 mg) were used as additives to prepare the biochar. Then, we injected 0.13 mol of solid $CaCl_2$ to each solution, maintaining the mixture at 30 °C, and stirred it at 600 rpm for 2 h to form sodium alginate gel beads. The gel beads were washed with ethanol (≥ 99.7%) and dried at 60 °C for 24 h before pyrolysis. Pyrolysis was conducted in a tube furnace for 2 h under an N_2 atmosphere at 400 °C. The model biochar (Mb) was washed three times with a 0.10 mol L^{-1} dilute hydrochloric acid solution to eliminate any DOM derived from the biochar. The pH was then adjusted to around 7.0, followed by drying the samples in an oven at 60 °C. The Mb samples were named according to the amount of graphene added (Mb-G0, Mb-G10, Mb-G20, and Mb-G40).

Fourier transform infrared spectroscopy (FTIR) was used to determine the surface functional groups of Mb (Vertex 80-Hyperion 2000). The conductivity of Mb was measured using a powder resistivity analyser (ST2722-SZ, Jingge, China). The surface area of Mb was determined based on the Brunauer–Emmett–Teller (BET) method using a surface area analyser (BSD-PM1, Beiteshi, China). The electron donating capacity (EDC) and electron accepting capacity (EAC) of Mb were evaluated through mediated electrochemical oxidation and reduction methods using an electrochemical workstation (IGS1130, Yingke, China). The working, counter, and reference electrodes were a glass carbon pool (50 mL), Pt wire, and Ag/AgCl electrodes, respectively. The electron shuttle agent, 2,2′-azide-bis (3-ethylbenzothiazolin-6-sulfonic acid) diammonium salt (>98%) or diquat dibromide monohydrate, were introduced into a PBS solution (0.1 mol L^{-1}) to induce current peaks under a N_2 atmosphere at potentials of 0.61 V or − 0.49 V.

2.2 Soil incubation experiment

The paddy soil for the experiment was collected from Jianshui, Yunnan, China, and stored in a blue-lid bottle (1 L) to avoid light exposure. For the control group, 6 g of paddy soil was placed in a 20 mL reagent bottle. For the experimental groups, 90 mg of different Mb samples was added to the paddy soil in separate reagent bottles. Subsequently, 6 mmol of ethanol was added to each bottle as carbon source, the headspace was flushed with N_2, and all bottles were incubated at 30 °C. CH_4 and CO_2 concentrations during incubation were determined using a gas chromatograph (9790, Fuli, China).

At the end of the test, the paddy soil was transferred to a centrifuge tube for high-speed centrifugation (12,000 rpm, 15 min, 4 °C) to separate the supernatant from the bottom peat mixture. Dissolved organic matter (DOM) in the paddy soil was collected from the supernatant using a 0.45 μm filter membrane. The total organic carbon (TOC) concentration in the supernatant was determined using a TOC analyser (Vario TOC Element, Germany) to represent the DOM concentration in the paddy soil. Excitation-emission matrix (EEM) spectra was employed to investigate the diversity in DOM composition. Emission scans spanned from 250 to 550 nm, and excitation wavelengths ranged from 200 to 450 nm using a fluorescence spectrophotometer (LS55, Perkin Elmer).

2.3 ETR of paddy soil

When the CH_4 concentration produced by the paddy soil stabilised, a three-electrode system was assembled with glass carbon, Pt wire, and Ag/AgCl electrodes as the working, counter, and reference electrodes, respectively (Kluepfel et al. 2014). Cyclic voltammetry (CV) curves

for all the paddy soil samples were obtained using an electrochemical workstation (IGS1130, Yingke, China). The potential range was −0.8 V to 0.4 V, and the potential scanning rate ranged from 20 to 200 mV s^{-1}. Based on the oxidation and reduction peaks in the CV curve, the ETR (*k*, mol e^- s^{-1}) was calculated as follows:

$$k = \frac{\int_0^t \mathrm{Idt}}{\mathrm{T}} \quad (1)$$

where *k* is the ETR of the paddy soil, I (A) denotes the real-time current, and t (s) is the duration of the CV result. ∫Idt (mol e^-) indicates the total electron transfer capacity, which is obtained from integrating the oxidation/reduction peak in CV curves, and T (s) represents the scan time of the oxidation or reduction peak.

After testing, the supernatant of the paddy soil was separated by centrifugation. An equal volume of ultrapure water was added to the paddy soil, and the mixture was vigorously shaken for 1 h at 30 °C in the dark. This procedure was repeated eight times to reduce the influence of dissolved organic matter on the CV analysis. Mb was introduced into ultrapure water at a concentration of 6 g L^{-1} for the CV test. Chloride (Cl^-), potassium (K^+), sodium (Na^+), ferrous (Fe^{2+}), phosphate (PO_4^{3-}), and sulphate (SO_4^{2-}) ions at concentrations of 10, 100, and 1000 mg L^{-1} were also added to the electrolyte in the three-electrode system for the CV test.

2.4 The electron accumulation of paddy soil

When the CH_4 production reached a stable level, 1 mL of the soil suspension was extracted and mixed with potassium ferricyanide solution (10 mmol L^{-1}, 54 mL). A 3 mol L^{-1} NaCl solution was used as the supporting electrolyte. After 24 h of oscillation and reaction, the mixture was analysed using a high-precision hydrodynamic electrochemical technique with a rotating disk electrode (RDE) (Prévoteau et al. 2016). The oxidation current observed in the hydrodynamic CV diagram was used to calculate the numbers of excess and unused electrons in the paddy soil. The electron accumulation in the paddy soil was quantified by measuring the final ferrocyanide yield using the following formulae:

$$Q_{ED} = \frac{nV[\mathrm{Ferro}]}{m} \quad (2)$$

$$[\mathrm{Ferro}] = \frac{j_{\mathrm{Ferro}}}{0.62nFD_{\mathrm{Ferro}}^{2/3}v^{-1/6}\omega^{1/2}} \quad (3)$$

where Q_{ED} (mol e^- (g soil C)$^{-1}$) represents the accumulated electron number in the paddy soil, n (1 mol) is the number of electrons for each mole of ferrocyanide reduced, V (55 mL) is the volume of solution, m (0.088 g) is the mass of dry soil C, and [Ferro] (mol L^{-1}) is the ferrocyanide concentration. F (96,485 C mol^{-1}) is the Faraday constant, D_{Ferro} (4.27×10^{-6} cm^2 s^{-1}) is the diffusion coefficient of ferrocyanide at 30 °C, ν (9.83×10^{-3} cm^2 s^{-1}) is the kinematic viscosity of 3.00 mol L^{-1} NaCl solution at 30 °C, and ω (4000 rpm) is the RDE rotation speed.

2.5 Microbial community analysis

After the CH_4 production reached a stable level, the microbial community was measured and analysed. Microbial diversity has primarily been studied in the conserved region of the nucleic acid sequence encoding ribosomal RNA. The 16S region, which represents the DNA sequence encoding the small subunit rRNA of the prokaryotic ribosome (16S rRNA), is commonly used in bacteria. In this study, 16S rRNA high-throughput sequencing was conducted using the Illumina NovaSeq sequencing platform, and paired-end sequences were constructed for sequencing. Species annotation and abundance analysis were performed by read splicing (using Usearch v10 software), filtering (using Trimmomatic v0.33 software), clustering, and denoising (using QIIME2 2020.6 software) to reveal the species composition of the samples and to analyse the species diversity among them. The analyses were conducted using Biomarker Technologies.

2.6 Mb and AQDS experiment

Anthraquinone-2,6-disulfonate (AQDS), a widely used analogue for quinone- and hydroquinone-containing molecules in DOM, has good electrochemical properties and can effectively simulate the electron transfer process of DOM in paddy soil. Thus, we utilized AQDS to construct a co-mediated electron-transfer system involving biochar and AQDS. Specifically, 2 mg Mb was added to the AQDS solution at an initial concentration of 5 mmol L^{-1}. The CV curves of the samples were measured using the same electrochemical workstation, with a voltage range of −0.6 V to 1.6 V and a potential scanning speed ranging from 100 to 800 mV s^{-1}.

3 Results and discussion

3.1 Methane generation from paddy soil

The conductivity of the Mb material gradually increased with the addition of graphene. Specifically, Mb-G0 exhibited low conductivity (4.08×10^{-10} S cm^{-1}); however, the graphene modification dramatically increased the conductivity to 0.43 S cm^{-1} for Mb-G40 (Fig. 1). The FTIR results showed that the peak positions and intensities of the surface functional groups of these Mb materials were similar (Figure S1a), indicating that the addition of graphene did not significantly alter their surface functional

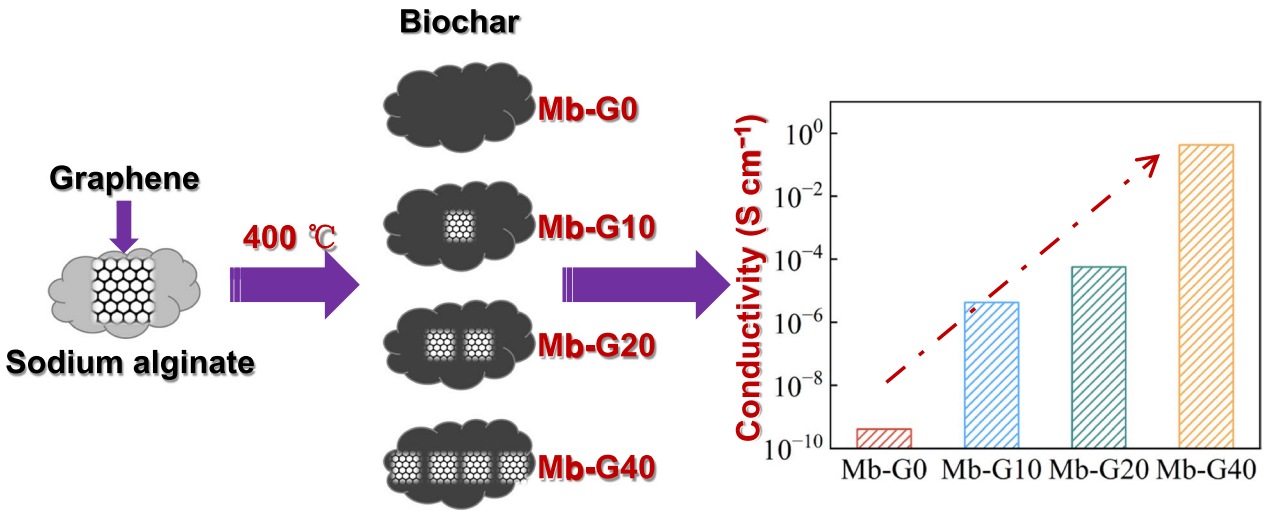

Fig. 1 Preparation of a series of Mb samples with various conductivities

groups. The particle size of the Mb material ranged from 27.51 to 103.53 μm, decreasing gradually with increasing graphene content (Figure S1b). Moreover, Mb samples with higher graphene contents exhibited larger specific surface areas, which increased from 47.90 $m^2\ g^{-1}$ (Mb-G0) to 94.44 $m^2\ g^{-1}$ (Mb-G40) (Figure S1c).

Mb samples were added to the paddy soil, and CH_4 accumulation in the paddy soil system was analysed using gas chromatography (Fig. 2a). The CH_4 generated from the paddy soil increased gradually and then stabilised over the 16-day incubation period. Notably, CH_4 accumulation in all paddy systems supplemented with Mb was significantly higher than in the paddy soil without Mb (control). Specifically, CH_4 accumulation in paddy soil system supplemented with Mb-G40 reached 3.45 ± 0.12 mmol, which was 69% higher than that in the control (2.04 ± 0.06 mmol). CH_4 accumulation increased by 18–26% in the other Mb systems compared to that in the control. This suggests that biochar addition can enhances CH_4 production in paddy soils.

The DOM concentration was determined by measuring the TOC content in the supernatant of the paddy soil (Fig. 2b). Before incubation, the DOM concentration in the paddy soil was 14.02 ± 0.05 g L^{-1}. After

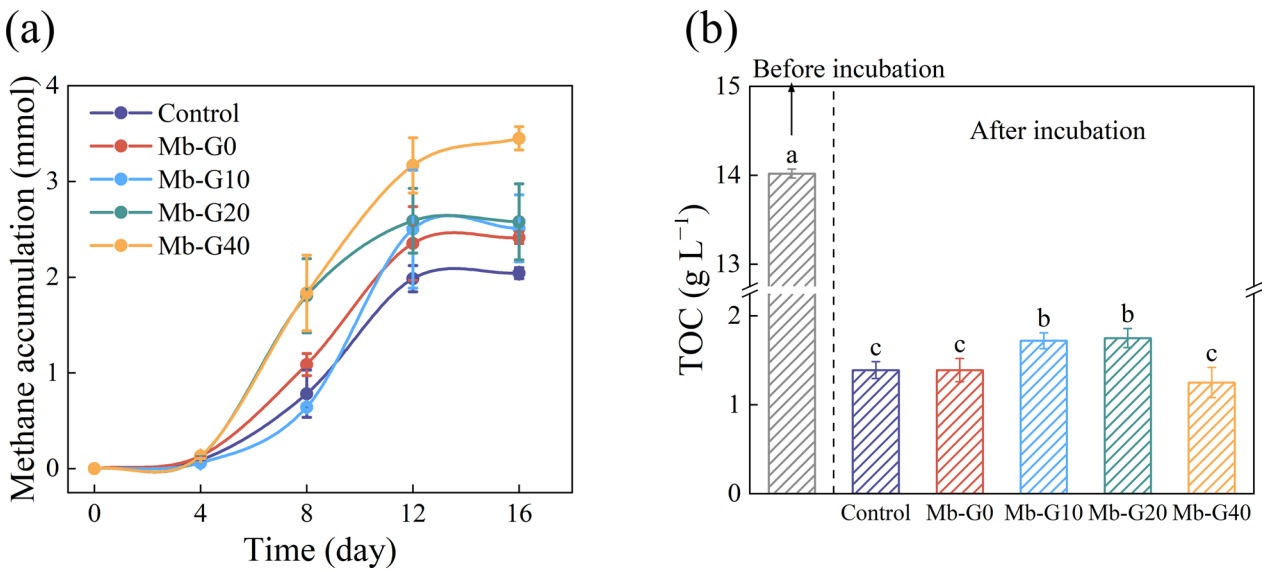

Fig. 2 Methane accumulation of paddy soil with and without Mb (**a**); TOC concentration of paddy soil before incubation and TOC concentration of paddy soil after incubation with and without Mb (**b**) (different letters indicate significant difference at $p < 0.05$)

over 16 days of incubation, DOM concentrations significantly decreased to 8.9–12.5% of the initial levels. This suggests that DOM, which serves as a carbon and energy source for microorganisms in paddy soil, is decomposed by microorganisms into compounds essential for their growth and metabolism.

Compared to the control (1.39 ± 0.09 g L^{-1}), DOM concentrations in the Mb-G10 (1.72 ± 0.09 g L^{-1}) and Mb-G20 (1.75 ± 0.11 g L^{-1}) systems showed slight increases, whereas the DOM concentration in the Mb-G40 system (1.25 ± 0.17 g L^{-1}) was comparable to that of the control. For instance, in the Mb-G40 system, DOM was likely adsorbed by Mb-G40 because of its large specific surface area, leading to a lower DOM consumption than in the control. However, methane production in the control system was significantly lower than that in the Mb-G40 system. After analyzing the DOM concentration, we examined the composition of the DOM samples. Five components were consistently identified in all DOM samples (Figure S2, Table S1). The composition of all DOM samples exhibited a high level of similarity based on fluorescence intensity, predominantly comprising humic acid-like and fulvic acid-like substances.

3.2 Electron transfer in the paddy soil was mainly mediated by DOM

Following the soil incubation experiment, electrochemical tests were conducted on the paddy soils using CV analysis. Figure S3 displays the curves obtained at various scanning rates (ranging from 20 to 200 mV s^{-1}). At a consistent scanning rate of 200 mV s^{-1}, distinct oxidation and reduction peaks appeared at the potentials of 0.1 V and −0.2 V, respectively (Fig. 3a). Compared to those in the control, the peak currents in the paddy soil systems increased after the application of Mb. More precisely, the absolute value of the reduction peak current in the Mb-G40 group was 213.5 ± 12.5 μA, approximately three times that of the control (71.8 ± 13.4 μA). As the conductivity of the Mb samples increased, the electrochemical response of the paddy soil system increased.

We mixed Mb with ultrapure water and scanned the CV curves at 200 mV s^{-1} (Figure S4a). No comparable peaks were observed at 0.1 V and −0.2 V. Additionally, the DOM derived from biochar used in this experiment was washed with ethanol and dilute hydrochloric acid during the preparation process, which excluded the influence of the DOM derived from biochar on the experimental results. A similar observation (Figure S4b) was made in solutions containing inorganic ions (Cl^-, K^+, Na^+, Fe^{2+}, PO_4^{3-}, and SO_4^{2-}) at concentrations

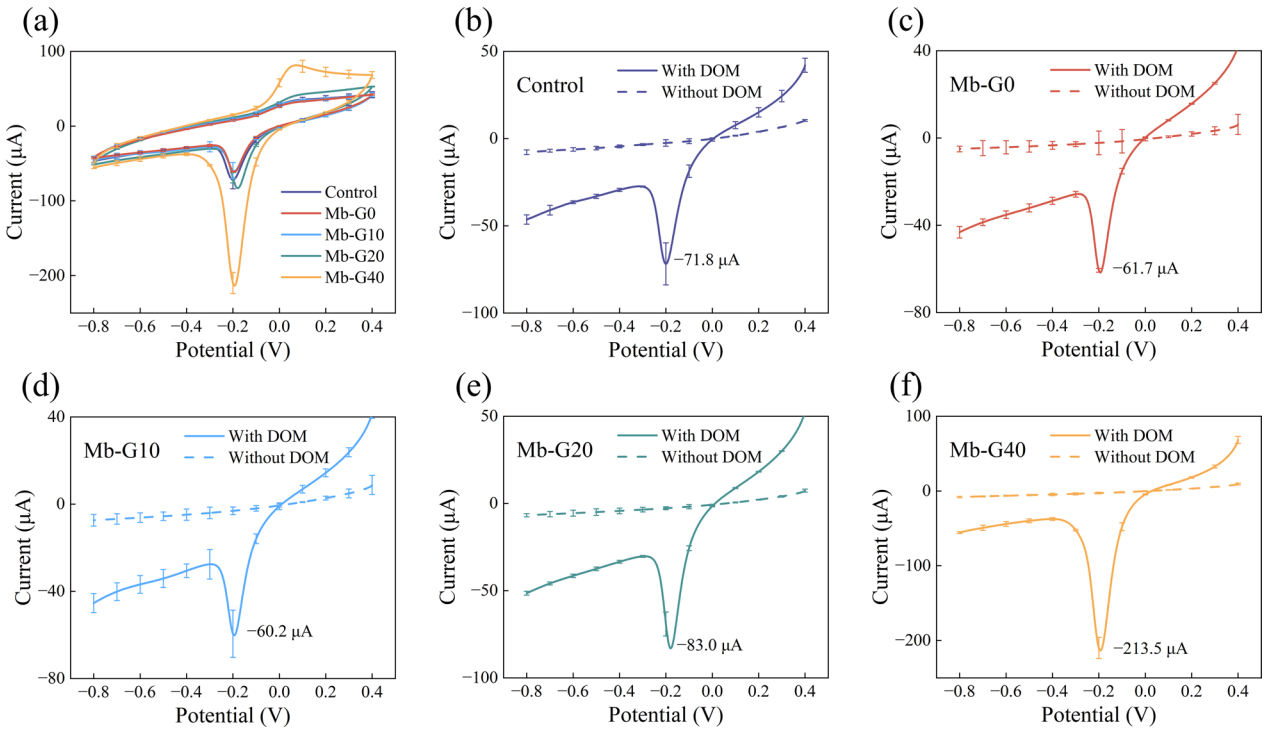

Fig. 3 CV curves of paddy soil with and without Mb at 200 mV s^{-1} (**a**); the reduction peaks of the CV curves before and after removing completely DOM from the paddy soil without Mb (**b**) and with Mb-G0 (**c**), Mb-G10 (**d**), Mb-G20 (**e**) and Mb-G40 (**f**)

significantly higher than those found in the paddy soil. Therefore, potential contributions of these inorganic ions to the CV peaks were excluded. DOM plays a significant role in electron transfer processes in soil and aquatic ecosystems (Bai et al. 2023). Sun et al. found that the electrochemical activity of DOM was significantly stronger than that of minerals, inorganic ions, metal ions, and microorganisms in soil (Sun et al. 2021). In conclusion, we speculate that the addition of Mb to this experimental system influences the electron transfer process of DOM in the soil, thereby affecting CH_4 production.

To validate our hypothesis, we tested the CV curves of all the experimental groups after the complete removal of DOM (Figure S5). In all systems, the soil without DOM had no reduction peaks comparable to the results before DOM removal (Fig. 3b–f). These results indicate that the redox peaks observed in the CV curves were primarily due to the redox process of DOM, which is the main factor mediating redox reactions in paddy soil systems.

In a system with the addition of the same amount of Mb, when the scanning rate was gradually increased from 20 to 200 mV s^{-1}, the oxidation and reduction peaks shifted towards positive and negative potentials, respectively (Figure S3). For Mb-G40, the peak potential difference increased from 212 to 258 mV. The analysis revealed a strong linear relationship between the peak current and square root of the potential scanning rate (Figure S6a), confirming that the electrons transferred through the surface of the working electrode were controlled by the diffusion of substances in the paddy soil. Based on previous studies, this substance was identified as DOM. Further calculations showed a strict linear correlation between the peak potential and the square root of the potential scanning rate (Figure S6b), indicating that the redox reaction in the paddy soil was quasi-reversible (Sun et al. 2017).

3.3 Increased methane production was due to higher conductivity of Mb

ETR in the paddy soil system was calculated using a CV curve (Fig. 4a). The ETR in the paddy soil increased with the conductivity of the Mb samples. Specifically, the ETR of Mb-G40 ($(7.22 \pm 0.61) \times 10^{-4}$ μmol e^- s^{-1}) was significantly higher than that of the other paddy soil systems, approximately three times greater than that of the control ($(2.05 \pm 0.42) \times 10^{-4}$ μmol e^- s^{-1}). The conductivity of the Mb samples was positively correlated with the ETR in paddy soil ($r = 0.70$, $p < 0.05$) (Fig. 4b), indicating that the enhanced electron transfer in the paddy soil was mainly due to the conductivity of the Mb samples. This suggests that biochar particles may provide fast electron transfer tunnels in paddy soils through their conductivity (Liu et al. 2020).

Importantly, we observed a significant positive correlation between CH_4 production in paddy soils and ETR ($r = 0.85$, $p < 0.05$) (Fig. 4c), indicating that Mb enhances electron transfer through its conductivity, thus promoting methanogenic reactions and CH_4 generation. Furthermore, the BET surface areas of the Mb samples showed positive correlation with CH_4 accumulation ($r = 0.79$, $p < 0.05$) (Figure S7). The large specific surface area of biochar stores nutrients, provides a microenvironment for microorganisms, and offers more active sites for electron exchange among microorganisms, DOM, and Mb. Our findings align with previous research showing that increased surface area facilitates electron transfer during methanogenesis (Yu et al. 2015).

Previous research found no significant correlation between biochar conductivity and CH_4 generation in anaerobic cultures using ethanol as a substrate (Yuan et al. 2018). Their conductivity range (2.25 ± 0.06–28.53 ± 0.86 μS cm^{-1}) was significantly narrower than the gradient conductivity spectrum evaluated in this study (4.08×10^{-10}–0.43 S cm^{-1}). This limited range may hinder the detection of conductivity-dependent effects on methanogenesis. In contrast, the broader conductivity range of biochar in this study facilitated the identification of its impact on methanogenesis.

In addition to archaea in methanogenesis, other substances in paddy soils, including DOM and minerals, can restore electrons (Sun et al. 2021). We quantified the electron accumulation in the paddy soil by measuring the increase in the electron-supplying capacity of the paddy soil using hydrodynamic CV (Figs. 4d and S8). Compared with that in the control (43.4 ± 0.2 μmol e^- (g soil C)$^{-1}$), the addition of Mb increased the electron accumulation in paddy soil. Electron accumulation increased with increasing Mb conductivity. Specifically, the highest accumulated electrons were observed in Mb-G40 (52.5 ± 0.4 μmol e^- (g soil C)$^{-1}$), followed by Mb-G20 (49.9 ± 0.2 μmol e^- (g soil C)$^{-1}$), Mb-G10 (48.9 ± 0.1 μmol e^- (g soil C)$^{-1}$), and Mb-G0 (46.7 ± 0.3 μmol e^- (g soil C)$^{-1}$). The EDC of Mb ranged from 1.78 ± 0.06 to 4.27 ± 0.80 mmol e^- (g biochar)$^{-1}$ across different graphene contents (Mb-G40 to Mb-G0) (Figure S9a–d). Similarly, the EAC of Mb varied from 0.23 ± 0.04 to 0.53 ± 0.05 mmol e^- (g biochar)$^{-1}$ for the same graphene content range (Mb-G40 to Mb-G0) (Figure S9e–h). The increase in graphene content led to a gradual decrease in both EDC and EAC of Mb, indicating that the enhanced ETR observed in soil incubation experiments was not due to the biochar redox reaction. Instead, the parallel trends between ETR in paddy soil and the biochar conductivity suggest that the accelerated electron transfer in the soil was primarily due to its conductivity. This aligns with the findings of Sun et al. (2017), who proposed that the primary mechanism

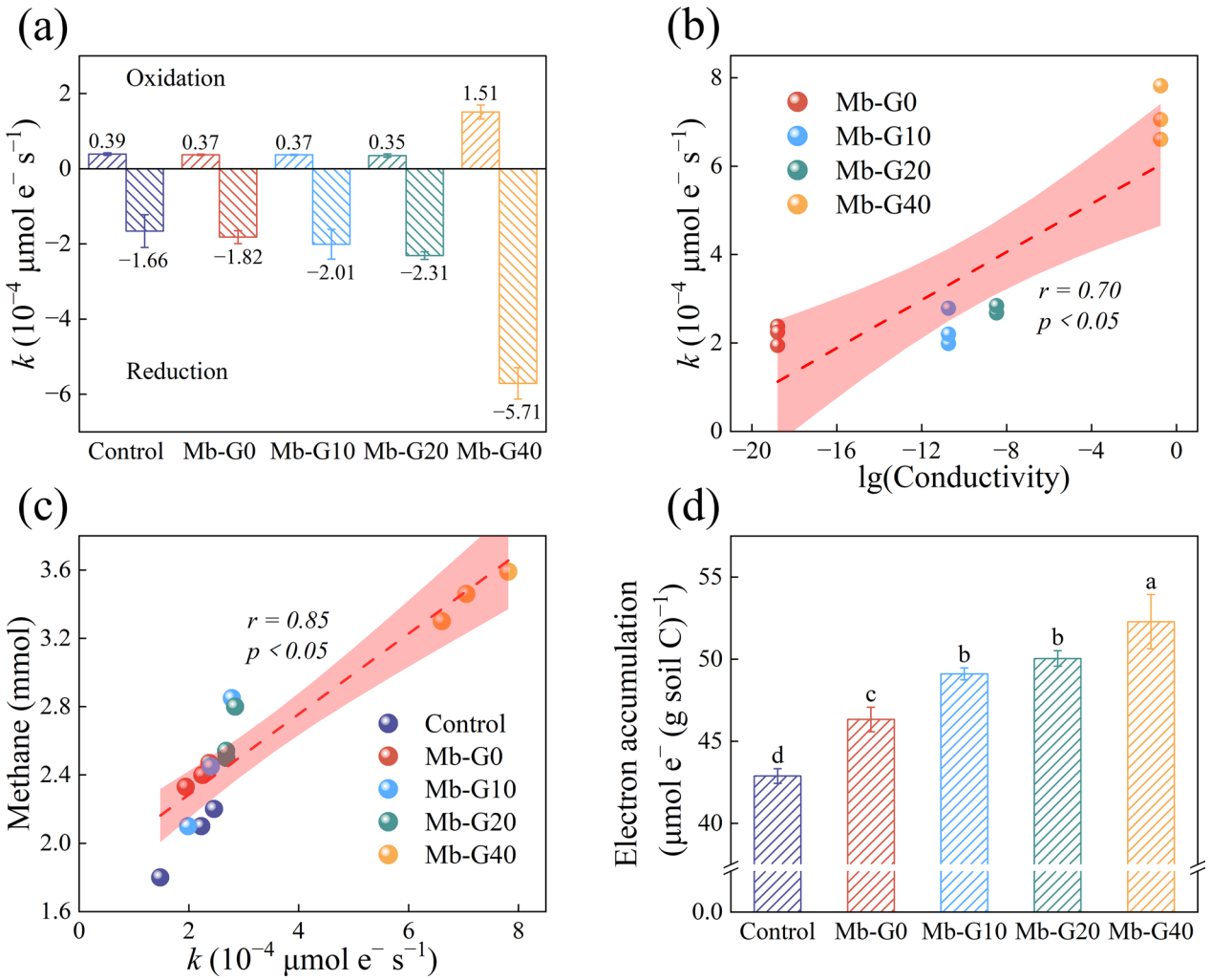

Fig. 4 The ETR of paddy soil with and without Mb (**a**); linear correlation between logarithm of Mb conductivity and ETR of paddy soil with Mb (**b**); linear correlation between methane accumulation and ETR of paddy soil (**c**); the electron accumulation of paddy soil with Mb and without Mb (**d**) (different letters indicate significant difference at $p < 0.05$)

of electron transfer in high-temperature biochar is conductive electron transfer.

These studies indicated that the electron transfer process in paddy soils is primarily driven by DOM diffusion. Our study reveals that conductive biochar actively participates in DOM-mediated electron transfer, with its conductivity being crucial. High electrical conductivity in biochar (such as Mb-G40 with 0.43 S cm^{-1}) significantly accelerates electron transfer through both biochar and DOM. The interactions between biochar and DOM are crucial to this process. Variations in the DOM adsorption mechanisms on biochar and the compositional changes of DOM upon adsorption influence electron transfer dynamics. Therefore, biochar effectively accelerated the electron transfer in the paddy soil (Fig. 5), resulting in the generation of more methane.

The relationship between ETR and methane production is context-dependent, influenced by two critical factors: the availability of electron donors and the presence of competing electron acceptors. The primary issue is whether sufficient carbon sources (electron donors) exist within the system (Luo et al. 2022; Rao et al. 2017). Even with increased ETR, methane production is constrained by the low concentration of DOM. Insufficient DOM limits substrate decomposition and fails to supply adequate electrons, so higher ETR does not necessarily enhance methane production. Additionally, competition from alternative electron acceptors, such as sulfate, poses a challenge (Luo et al. 2023; Zhao et al. 2021). Sulfate-reducing bacteria can outcompete methanogens through preferential electron capture, thereby suppressing methanogenesis even with a substantial increase in ETR. Thus,

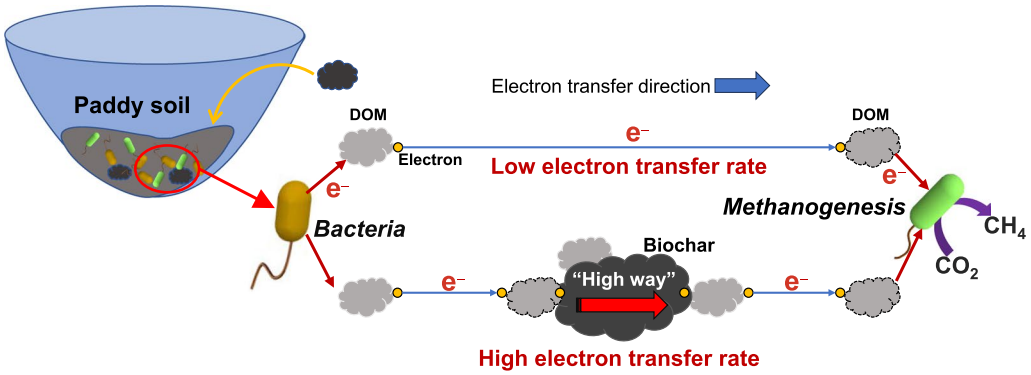

Fig. 5 Mechanism of the electron transfer process with DOM and Mb in paddy soil

there is no straightforward correlation between ETR and methane production in these contexts.

3.4 Model biochar and AQDS experiment

To verify the enhanced effect of Mb on electron transfer mediated by DOM, we used AQDS as a model material for DOM and conducted electrochemical experiments with AQDS and Mb samples. The adsorption capacity of Mb for AQDS over time is shown in Fig. 6a. When the adsorption equilibrium was reached, compared with that of the control (0.08 ± 0.05 mmol L^{-1}), the AQDS concentration of Mb-G40 system under adsorption equilibrium was 1.40 ± 0.05 mmol L^{-1}, representing the highest in all experimental groups. This result indicates that as the graphene content increased, coupled with changes in the Mb surface area, the larger surface area and rich pore structure of Mb facilitated more effective adsorption of AQDS.

Once the AQDS adsorption by Mb reached equilibrium, the CV curves of the experimental group were measured using the same three-electrode system (Figs. 6b, c and S10). The CV curves exhibited distinct oxidation and reduction peaks at 0.0 V and − 0.7 V, respectively, which aligns with the results of a previous study (Bai et al. 2020). Despite the decrease in the AQDS concentration, the electrochemical response of the system increased after adsorption equilibrium with Mb-G40 addition. The oxidation peak current of Mb-G40 (117.25 μA) was higher than that of the control (103.80 μA), followed by Mb-G20 (110.70 μA). The oxidation peak current of Mb-G10 (96.67 μA) was the lowest among all groups. The CV curves of the pure Mb samples were also obtained (Fig. 6b, c), and no peaks were observed at the same potential. These results demonstrate that Mb adsorbed AQDS and accelerated electron transfer in the system in conjunction with AQDS. Based on the oxidation and reduction peaks in the CV curves, we calculated the ETR of the Mb/AQDS systems (Fig. 6d). We found that the ETR in the systems gradually increased with increasing Mb conductivity, and the oxidation (6.33 ± 0.04 μmol e^- (s mol AQDS)$^{-1}$) and reduction rates (− 7.38 ± 0.04 μmol e^- (s mol AQDS)$^{-1}$) of the Mb-G40 group were significantly higher than those of other groups. In contrast, the oxidation (4.33 ± 0.06 μmol e^- (s mol AQDS)$^{-1}$) and reduction rates (− 5.78 ± 0.08 μmol e^- (s mol AQDS)$^{-1}$) Mb-0 were almost identical to those of the control (4.08 ± 0.03 μmol e^- (s mol AQDS)$^{-1}$ and − 5.42 ± 0.04 μmol e^- (s mol AQDS)$^{-1}$). This indicates that the increase in Mb conductivity accelerated the ETR mediated by AQDS in solution, which is consistent with the conclusion that Mb can mediate electron transfer facilitated by DOM in paddy soil.

We also found that the ETRs of the soil incubation experimental groups were lower than those of the Mb and AQDS experimental groups. This may be because the Mb and AQDS experiments used AQDS as the simulated DOM substance. Pure AQDS is rich in quinone functional groups, which can effectively mediate electron transfer in the system. Furthermore, the Mb and AQDS experimental systems only had AQDS and Mb, resulting in less interference and, consequently, a higher ETR. However, DOM in soil is a complex mixture comprising functional groups such as amino acids, aromatics, and aliphatic groups containing O, N, and S, as well as components that can effectively mediate electron transfer (Aeschbacher et al. 2010; Walpen et al. 2018). Therefore, electron transfer in the soil incubation experiments was likely hindered by the presence of soil inorganic ions, metal ions, and organic compounds. We also found that the ETR of Mb-G40 in the soil incubation experiment was significantly larger than that of the other groups, whereas in the Mb and AQDS experiments, the ETR of Mb-G40 was not much higher than that of the other groups. This difference may be related to the substantial enhancement in biochar conductivity. A drastic increase in biochar conductivity can lead to qualitative changes in

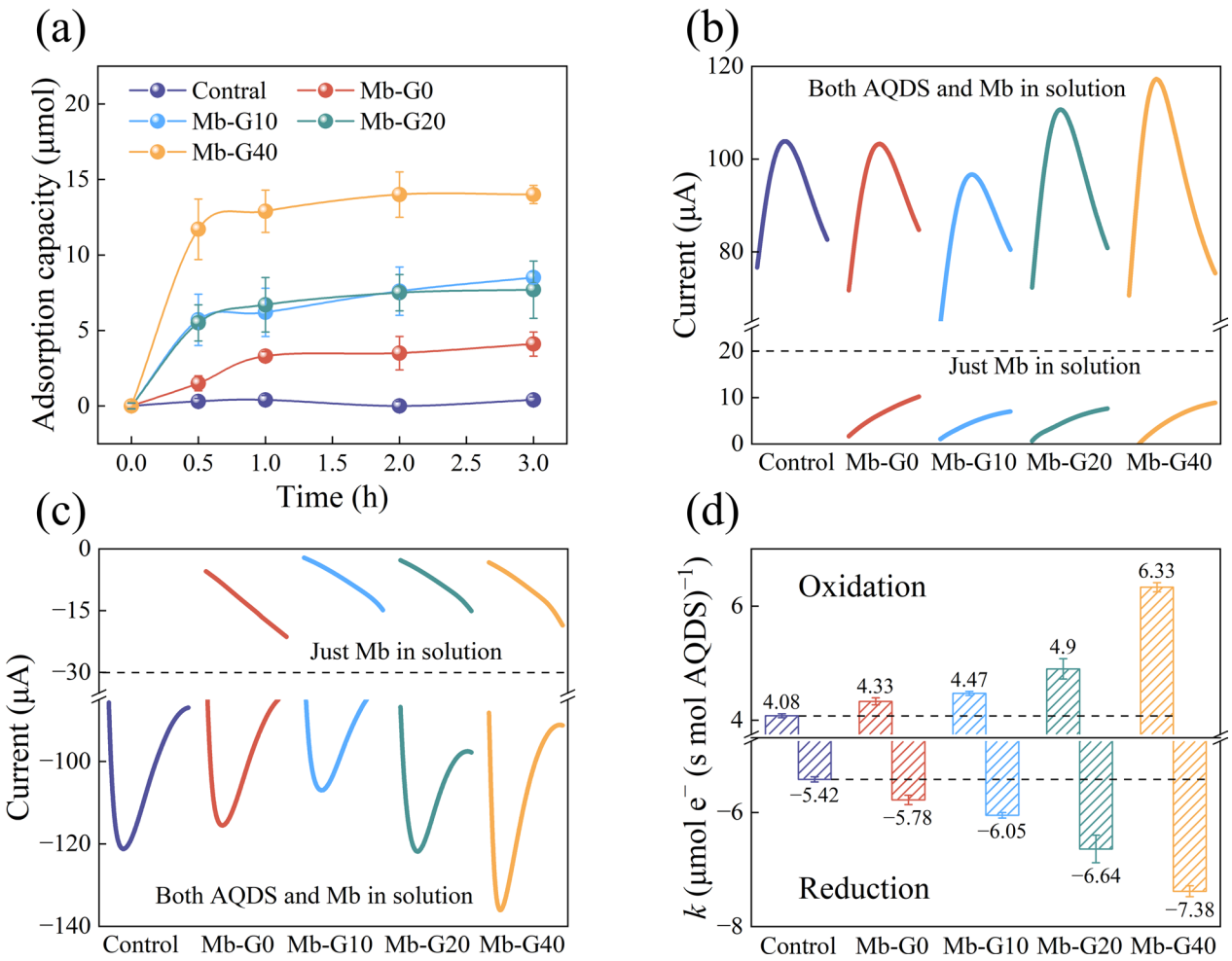

Fig. 6 The adsorption curves of AQDS without Mb (control) and with Mb-G0, Mb-G10, Mb-G20 and Mb-G40 (**a**); oxidation peak (**b**) and reduction peak (**c**) in the CV curves of just Mb in solution and both AQDS and Mb in solution at the scan rate of 800 mV s^{-1}; the ETR of AQDS with and without Mb addition (**d**)

various reactions of the paddy soil, significantly enhancing electron transfer within the paddy soil system and increasing the ETR.

3.5 Analysis of microbial community structure

This study evaluated the microbial community of the system at the end of cultivation, a stage where CH_4 production in the system stabilised and substrate hydrolysis and acidification were largely completed (Kim et al. 2017). Following the addition of Mb, the Chao1 and Shannon indices of the bacterial community decreased compared with those of the control, whereas the indices for the archaeal community increased (Figure S11). Previous research has indicated that bacteria primarily contribute to CH_4 production through substrate hydrolysis and acidification, whereas archaea are more active in the methanogenic stage (Park et al. 2018). Our findings suggest that the addition of Mb alters the abundance of bacterial and archaeal communities in paddy soil systems (Amin et al. 2021). Theoretically, for the same ethanol content, methane generation by acetoclastic methanogenesis is lower than that by electron or hydrogenotrophic methanogenesis (Chen et al. 2022). We hypothesized that incorporating biochar into paddy soil systems alters the archaeal microbial community, facilitating a shift from acetoclastic to electron and hydrogenotrophic methanogenesis. This transition reduces carbon source consumption while increasing methane production (Jiang et al. 2022).

The composition of bacterial and archaeal species at the genus level are shown in Fig. 7a, b, respectively. *Clostridium* was the dominant bacterial genus across all experimental systems, with a relative abundance ranging from 14.5% to 27.2%. This genus primarily contributes to the hydrolysis and acidification of organic matter (Kim et al. 2017; Verma et al. 2021). *Geobacteraceae*, a crucial species involved in hydrolysis and acidification,

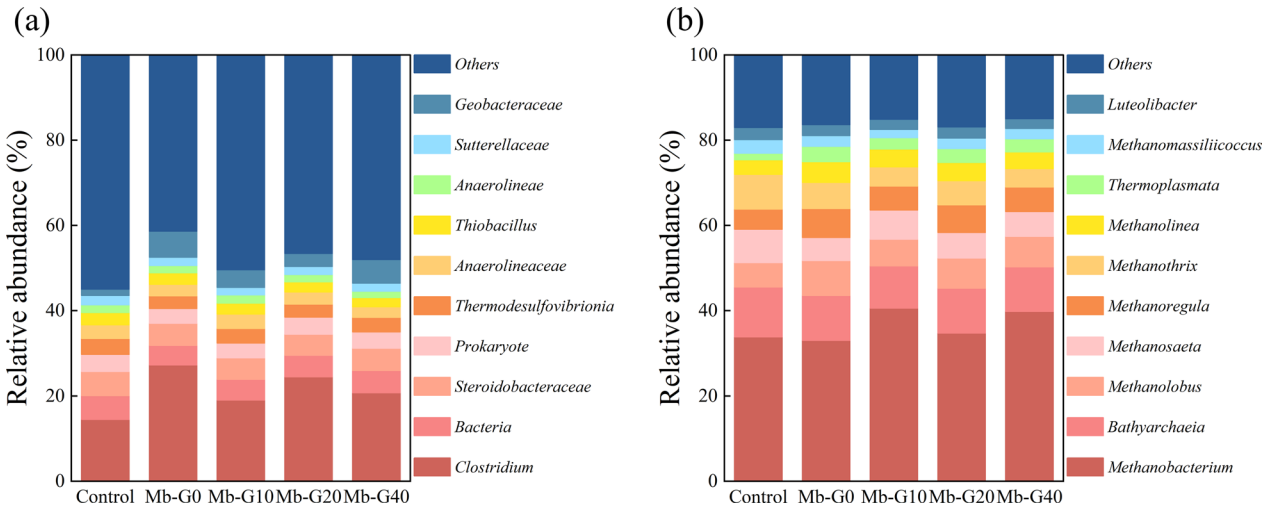

Fig. 7 The relative abundances of the top 10 genera identified in the bacteria (**a**) and archaeal (**b**) communities

can oxidise acetic acid and transfer electrons to methanogenic archaea (Ali et al. 2019). The abundance of *Geobacteraceae* in paddy soils amended with Mb (ranging from 3.0 to 6.1%) was notably higher than that in the control (1.4%). We hypothesised that the addition of Mb to paddy soil enhances electron transfer from *Geobacteraceae* to archaea, thus promoting methanogen growth and increasing CH_4 production.

In this study, *Methanosaeta* and *Methanothrix* were two common species capable of utilising acetic acid for energy and CH_4 production (Holmes and Smith 2016; Verma et al. 2021), and their abundance in paddy soil without Mb were 7.8% (*Methanosaeta*) and 8.1% (*Methanothrix*), which was significantly higher than that in paddy soil with Mb addition (5.4–6.8%, *Methanosaeta*; 4.3–6.1%, *Methanothrix*). This indicated that the contribution of acetoclastic methanogenesis was higher in the control group. Meanwhile, *Methanobacterium*, the primary methanogenic archaea in paddy soil systems, is a prevalent hydrogenotrophic methanogen that uses H_2 as an electron shuttle to reduce CO_2 to CH_4 (Park et al. 2018; Rotaru et al. 2014). Additionally, *Methanobacterium* can directly accept electrons through direct interspecific electron transfer to reduce CO_2 to CH_4 (Verma et al. 2021). Compared with the control (33.0%), the abundance in the paddy soil supplemented with Mb increased from 33.8 to 40.6%. Additionally, *Methanoregula*, *Methanolobus*, and *Methanolina* are all electron and hydrogenotrophic methanogenic archaea (Holmes and Smith 2016), and their abundance increased in the paddy soil after the addition of Mb. The variations in archaeal abundance indicate a shift in the CH_4 production pathway from acetoclastic to electron and hydrogenotrophic methanogenesis following the addition of Mb, supporting our hypothesis from the DOM section.

However, we found no significant differences in the relative abundance of other archaeal species across the Mb treatments from Mb-G0 to Mb-G40. This lack of significant change could be attributed to the relatively short incubation period during which the community structure may not have undergone substantial shifts. Biochar and DOM can both function as electron shuttles, facilitating electron transfer between bacteria and archaea and thereby promoting CH_4 generation (Zhang et al. 2021). Our results confirmed that the addition of biochar enhanced the electrochemical activity of DOM in the system, leading to more active microbial growth and, consequently, increased CH_4 production. The effectiveness of this enhancement depends on the conductivity of biochar.

4 Conclusion

Biochar samples with different conductivities were prepared by incorporating varying amounts of graphene. The samples were applied to a paddy soil system to assess the effects of biochar conductivity on CH_4 production. The results showed that CH_4 yield in paddy soil increased with higher biochar conductivity, independent of the methanogenic archaeal community, primarily due to enhanced ETR within the system. Biochar conductivity intensified ETR facilitated by DOM. This conclusion was further validated through experiments using biochar and AQDS, which are model compounds for DOM. This study provides valuable insights into the mechanisms by which biochar conductivity influences methanogenesis in paddy soils, and offers a theoretical basis for evaluating

the effects of biochar on greenhouse gas emission, particularly in paddy soil ecosystems.

Supplementary Information

The online version contains supplementary material available at https://doi.org/10.1007/s42773-025-00478-8.

Additional file 1.

Acknowledgements
We appreciated the support from the Yunnan Provincial Science and Technology Project at Southwest United Graduate School (202302 AP370002), National Natural Science Fund of China (42277236), Yunnan Fundamental Research Projects (202201BE070001-012), and Yunnan Major Scientific and Technological Projects (202202 AG050019).

Author contributions
All authors contributed to the study conception and design. Conceptualization, material preparation, methodology, supervision, validation, visualization, writing-original draft, writing-review & editing were performed by Yufei Wu; Material preparation and data collection were performed by Ting He; Methodology was performed by CC; Data analysis was performed by Bo Liu; Project administration was performed by Zhaofeng Chang; Validation was performed by Wei Du; Visualization was performed by Hao Li; Methodology, project administration, supervision, validation, visualization, funding acquisition, and writing-review & editing were performed by Peng Zhang; Methodology, project administration, supervision, and writing-reviewing & editing were performed by Bo Pan. And all authors commented on previous versions of the manuscript. All authors read and approved the final manuscript.

Funding
This work was supported by the Yunnan Provincial Science and Technology Project at Southwest United Graduate School (202302 AP370002), National Natural Science Fund of China (42277236), Yunnan Fundamental Research Projects (202201BE070001-012), and Yunnan Major Scientific and Technological Projects (202202 AG050019).

Data availability
The datasets used or analyzed during the current study are available from the corresponding author on reasonable request.

Declarations

Competing interests
Bo Pan is an EBM of the journal Biochar, but he was not involved in the peer-review or handling of the manuscript. The authors have no other competing interests to disclose.

Author details
[1]Yunnan Provincial Key Laboratory of Soil Carbon Sequestration and Pollution Control, Faculty of Environmental Science & Engineering, Kunming University of Science & Technology, Kunming 650500, Yunnan, China. [2]Kunming Dianchi and Plateau Lakes Institute, Kunming 650500, China.

Received: 18 December 2024 Revised: 17 May 2025 Accepted: 19 May 2025
Published online: 24 June 2025

References

Aeschbacher M, Sander M, Schwarzenbach RP (2010) Novel electrochemical approach to assess the redox properties of humic substances. Environ Sci Technol 44(1):87–93. https://doi.org/10.1021/es902627p
Ali S, Hua BB, Huang JJ, Droste RL, Zhou QX, Zhao WX, Chen L (2019) Effect of different initial low pH conditions on biogas production, composition, and shift in the aceticlastic methanogenic population. Bioresour Technol 289:7. https://doi.org/10.1016/j.biortech.2019.121579
Amin FR, Khalid H, El-Mashad HM, Chen C, Liu GQ, Zhang RH (2021) Functions of bacteria and archaea participating in the bioconversion of organic waste for methane production. Sci Total Environ 763:21. https://doi.org/10.1016/j.scitotenv.2020.143007
Asadi H, Ghorbani M, Rezaei-Rashti M, Abrishamkesh S, Amirahmadi E, Chen CR, Gorji M (2021) Application of rice husk biochar for achieving sustainable agriculture and environment. Rice Sci 28(4):325–343. https://doi.org/10.1016/j.rsci.2021.05.004
Bai YG, Sun TR, Angenent LT, Haderlein SB, Kappler A (2020) Electron hopping enables rapid electron transfer between quinone–/hydroquinone-containing organic molecules in microbial iron(III) mineral reduction. Environ Sci Technol 54(17):10646–10653. https://doi.org/10.1021/acs.est.0c02521
Bai YG, Sun TR, Mansor M, Joshi P, Zhuang YL, Haderlein SB, Fischer S, Konhauser KO, Alessi DS, Kappler A (2023) Networks of dissolved organic matter and organo-mineral associations stimulate electron transfer over centimeter distances. Environ Sci Technol Lett 10(6):493–498. https://doi.org/10.1021/acs.estlett.3c00172
Cavali M, Libardi N Jr, Mohedano RD, Belli P, da Costa RHR, de Castilhos AB Jr (2022) Biochar and hydrochar in the context of anaerobic digestion for a circular approach: an overview. Sci Total Environ 822:16. https://doi.org/10.1016/j.scitotenv.2022.153614
Chen JQ, Zhang PS, Zhang JX, He YL, Tong YW (2022) Micro-nano magnetite-loaded biochar enhances interspecies electron transfer and viability of functional microorganisms in anaerobic digestion. ACS Sustain Chem Eng 10(8):2811–2821. https://doi.org/10.1021/acssuschemeng.1c08288
Ding Y, Liu YG, Liu SB, Li ZW, Tan XF, Huang XX, Zeng GM, Zhou L, Zheng BH (2016) Biochar to improve soil fertility. A review. Agron Sustain Dev 36(2):18. https://doi.org/10.1007/s13593-016-0372-z
Haris M, Hamid Y, Usman M, Wang L, Saleem A, Su F, Guo JK, Li YT (2021) Crop-residues derived biochar: synthesis, properties, characterization and application for the removal of trace elements in soils. J Hazard Mater 416:21. https://doi.org/10.1016/j.jhazmat.2021.126212
Holmes DE, Smith JA (2016) Biologically produced methane as a renewable energy source. In: Sariaslani S, Gadd GM (eds) Advances in applied microbiology, vol 97. Elsevier Academic Press Inc, San Diego, pp 1–61
Ji MY, Zhou L, Zhang SC, Luo G, Sang WJ (2020) Effects of biochar on methane emission from paddy soil: focusing on DOM and microbial communities. Sci Total Environ 743:9. https://doi.org/10.1016/j.scitotenv.2020.140725
Jiang Q, Wu P, Zhang XD, Zhang Y, Cui MH, Liu HB, Liu H (2022) Deciphering the effects of engineered biochar on methane production and the mechanisms during anaerobic digestion: surface functional groups and electron exchange capacity. Energy Convers Manag 258:11. https://doi.org/10.1016/j.enconman.2022.115417
Jin HY, He ZW, Ren YX, Tang CC, Zhou AJ, Chen F, Liang B, Liu WZ, Wang AJ (2022) Role and significance of co-additive of biochar and nano-magnetite on methane production from waste activated sludge: non-synergistic rather than synergistic effects. Chem Eng J 439:11. https://doi.org/10.1016/j.cej.2022.135746
Kim M, Kim BC, Choi Y, Nam K (2017) Minimizing mixing intensity to improve the performance of rice straw anaerobic digestion via enhanced development of microbe-substrate aggregates. Bioresour Technol 245:590–597. https://doi.org/10.1016/j.biortech.2017.09.006
Kim NK, Lee SH, Kim Y, Park HD (2022) Current understanding and perspectives in anaerobic digestion based on genome-resolved metagenomic approaches. Bioresour Technol 344:12. https://doi.org/10.1016/j.biortech.2021.126350
Kluepfel L, Keiluweit M, Kleber M, Sander M (2014) Redox properties of plant biomass-derived black carbon (biochar). Environ Sci Technol 48(10):5601–5611. https://doi.org/10.1021/es500906d
Kubaczynski A, Walkiewicz A, Pytlak A, Grzadziel J, Galazka A, Brzezinska M (2023) Application of nitrogen-rich sunflower husks biochar promotes methane oxidation and increases abundance of *Methylobacter* in nitrogen-poor soil. J Environ Manag 348:12. https://doi.org/10.1016/j.jenvman.2023.119324
Leigh JA, Albers SV, Atomi H, Allers T (2011) Model organisms for genetics in the domain Archaea: methanogens, halophiles, Thermococcales and Sulfolobales. FEMS Microbiol Rev 35(4):577–608. https://doi.org/10.1111/j.1574-6976.2011.00265.x

Liu BH, Guo WQ, Wang HZ, Si QS, Zhao Q, Luo HC, Ren NQ (2020) B-doped graphitic porous biochar with enhanced surface affinity and electron transfer for efficient peroxydisulfate activation. Chem Eng J 396:11. https://doi.org/10.1016/j.cej.2020.125119

Luo D, Li YY, Yao HY, Chapman SJ (2022) Effects of different carbon sources on methane production and the methanogenic communities in iron rich flooded paddy soil. Sci Total Environ 823:10. https://doi.org/10.1016/j.scitotenv.2022.153636

Luo L, Han XY, Wang KR, Xu YX, Xiong LQ, Ma JN, Guo ZX, Tang JW (2023) Nearly 100% selective and visible-light-driven methane conversion to formaldehyde via. single-atom Cu and $W^{\delta+}$. Nat Commun 14(1):13. https://doi.org/10.1038/s41467-023-38334-7

Makarova KS, Sorokin AV, Novichkov PS, Wolf YI, Koonin EV (2007) Clusters of orthologous genes for 41 archaeal genomes and implications for evolutionary genomics of archaea. Biol Direct 2:20. https://doi.org/10.1186/1745-6150-2-33

Mand TD, Metcalf WW (2019) Energy conservation and hydrogenase function in methanogenic archaea, in particular the genus *Methanosarcina*. Microbiol Mol Biol Rev 83(4):22. https://doi.org/10.1128/mmbr.00020-19

Matthews R, Wassmann R (2003) Modelling the impacts of climate change and methane emission reductions on rice production: a review. Eur J Agron 19(4):573–598. https://doi.org/10.1016/s1161-0301(03)00005-4

Nan Q, Wang C, Wang H, Yi QQ, Wu WX (2020) Mitigating methane emission via annual biochar amendment pyrolyzed with rice straw from the same paddy field. Sci Total Environ 746:9. https://doi.org/10.1016/j.scitotenv.2020.141351

Nan Q, Xin LQ, Qin Y, Waqas M, Wu WX (2021) Exploring long-term effects of biochar on mitigating methane emissions from paddy soil: a review. Biochar 3(2):125–134. https://doi.org/10.1007/s42773-021-00096-0

Nguyen BT, Trinh NN, Bach QV (2020) Methane emissions and associated microbial activities from paddy salt-affected soil as influenced by biochar and cow manure addition. Appl Soil Ecol 152:9. https://doi.org/10.1016/j.apsoil.2020.103531

Park JH, Kang HJ, Park KH, Park HD (2018) Direct interspecies electron transfer via conductive materials: a perspective for anaerobic digestion applications. Bioresour Technol 254:300–311. https://doi.org/10.1016/j.biortech.2018.01.095

Prévoteau A, Ronsse F, Cid I, Boeckx P, Rabaey K (2016) The electron donating capacity of biochar is dramatically underestimated. Sci Rep 6:11. https://doi.org/10.1038/srep32870

Qi FJ, Kuppusamy S, Naidu R, Bolan NS, Ok YS, Lamb D, Li YB, Yu LB, Semple KT, Wang HL (2017) Pyrogenic carbon and its role in contaminant immobilization in soils. Crit Rev Environ Sci Technol 47(10):795–876. https://doi.org/10.1080/10643389.2017.1328918

Qian HY, Zhu XC, Huang S, Linquist B, Kuzyakov Y, Wassmann R, Minamikawa K, Martinez-Eixarch M, Yan XY, Zhou F, Sander BO, Zhang WJ, Shang ZY, Zou JW, Zheng XH, Li GH, Liu ZH, Wang SH, Ding YF, van Groenigen KJ, Jiang Y (2023) Greenhouse gas emissions and mitigation in rice agriculture. Nat Rev Earth Environ 4(10):716–732. https://doi.org/10.1038/s43017-023-00482-1

Rao H, Chmidt LCS, Bonin J, Robert M (2017) Visible-light-driven methane formation from CO_2 with a molecular iron catalyst. Nature 548(7665):74–77. https://doi.org/10.1038/nature23016

Rotaru AE, Shrestha PM, Liu FH, Shrestha M, Shrestha D, Embree M, Zengler K, Wardman C, Nevin KP, Lovley DR (2014) A new model for electron flow during anaerobic digestion: direct interspecies electron transfer to Methanosaeta for the reduction of carbon dioxide to methane. Energy Environ Sci 7(1):408–415. https://doi.org/10.1039/c3ee42189a

Sun TR, Levin BDA, Guzman JJL, Enders A, Muller DA, Angenent LT, Lehmann J (2017) Rapid electron transfer by the carbon matrix in natural pyrogenic carbon. Nat Commun 8:12. https://doi.org/10.1038/ncomms14873

Sun T, Guzman JJL, Seward JD, Enders A, Yavitt JB, Lehmann J, Angenent LT (2021) Suppressing peatland methane production by electron snorkeling through pyrogenic carbon in controlled laboratory incubations. Nat Commun 12(1):9. https://doi.org/10.1038/s41467-021-24350-y

Thauer RK, Kaster AK, Seedorf H, Buckel W, Hedderich R (2008) Methanogenic archaea: ecologically relevant differences in energy conservation. Nat Rev Microbiol 6(8):579–591. https://doi.org/10.1038/nrmicro1931

Uchimiya M, Chang S, Klasson KT (2011a) Screening biochars for heavy metal retention in soil: role of oxygen functional groups. J Hazard Mater 190(1–3):432–441. https://doi.org/10.1016/j.jhazmat.2011.03.063

Uchimiya M, Wartelle LH, Klasson KT, Fortier CA, Lima IM (2011b) Influence of pyrolysis temperature on biochar property and function as a heavy metal sorbent in soil. J Agric Food Chem 59(6):2501–2510. https://doi.org/10.1021/jf104206c

Verma J, Kumar D, Singh N, Katti SS, Shah YT (2021) Electricigens and microbial fuel cells for bioremediation and bioenergy production: a review. Environ Chem Lett 19(3):2091–2126. https://doi.org/10.1007/s10311-021-01199-7

Walpen N, Getzinger GJ, Schroth MH, Sander M (2018) Electron-donating phenolic and electron-accepting quinone moieties in peat dissolved organic matter: quantities and redox transformations in the context of peat biogeochemistry. Environ Sci Technol 52(9):5236–5245. https://doi.org/10.1021/acs.est.8b00594

Wang MW, Zhao ZQ, Zhang YB (2021) Magnetite-contained biochar derived from fenton sludge modulated electron transfer of microorganisms in anaerobic digestion. J Hazard Mater 403:9. https://doi.org/10.1016/j.jhazmat.2020.123972

Xiao LL, Sun R, Zhang P, Zheng SL, Tan Y, Li JJ, Zhang YC, Liu FH (2019) Simultaneous intensification of direct acetate cleavage and CO_2 reduction to generate methane by bioaugmentation and increased electron transfer. Chem Eng J 378:10. https://doi.org/10.1016/j.cej.2019.122229

Xie QQ, Lu Y, Tang L, Zeng GM, Yang ZH, Fan CZ, Wang JJ, Atashgahi S (2021) The mechanism and application of bidirectional extracellular electron transport in the field of energy and environment. Crit Rev Environ Sci Technol 51(17):1924–1969. https://doi.org/10.1080/10643389.2020.1773728

Yang Z, Sun TR, Kleindienst S, Straub D, Kretzschmar R, Angenent LT, Kappler A (2021) A coupled function of biochar as geobattery and geoconductor leads to stimulation of microbial Fe(III) reduction and methanogenesis in a paddy soil enrichment culture. Soil Biol Biochem 163:13. https://doi.org/10.1016/j.soilbio.2021.108446

Yu LP, Yuan Y, Tang J, Wang YQ, Zhou SG (2015) Biochar as an electron shuttle for reductive dechlorination of pentachlorophenol by Geobacter sulfurreducens. Sci Rep 5:10. https://doi.org/10.1038/srep16221

Yuan HY, Ding LJ, Zama EF, Liu PP, Hozzein WN, Zhu YG (2018) Biochar modulates methanogenesis through electron syntrophy of microorganisms with ethanol as a substrate. Environ Sci Technol 52(21):12198–12207. https://doi.org/10.1021/acs.est.8b04121

Zhang P, Zhang JS, Sun ZY, He C, Pan B, Xing BS (2021) The conductivity and redox properties of pyrolyzed carbon mediate methanogenesis in paddy soils with ethanol as substrate. Sci Total Environ 795:7. https://doi.org/10.1016/j.scitotenv.2021.148906

Zhao L, Chen H, Yuan ZG, Guo JH (2021) Interactions of functional microorganisms and their contributions to methane bioconversion to short-chain fatty acids. Water Res 199:8. https://doi.org/10.1016/j.watres.2021.117184